OXFORD

SOT | Society of Toxicology
www.toxsci.oxfordjournals.org

TOXICOLOGICAL SCIENCES, 171(2), 2019, 473–484

doi: 10.1093/toxsci/kfz164
Advance Access Publication Date: July 31, 2019
Research Article

The Valosin-Containing Protein Protects the Heart Against Pathological Ca^{2+} Overload by Modulating Ca^{2+} Uptake Proteins

Shaunrick Stoll,*,† Jing Xi,* Ben Ma,*,‡ Christiana Leimena,* Erik J. Behringer,† Gangjian Qin,§ and Hongyu Qiu*,‡,1

*Division of Physiology, Department of Basic Sciences, School of Medicine, Loma Linda University, Loma Linda, California 92350; †Division of Pharmacology, Department of Basic Sciences, School of Medicine, Loma Linda University, Loma Linda, California 92350; ‡Center of Molecular and Translational Medicine, Institution of Biomedical Science, Georgia State University, Atlanta, Georgia 30303; and §Department of Biomedical Engineering, Molecular Cardiology Program, School of Medicine and School of Engineering, University of Alabama at Birmingham, Birmingham, Alabama 35294-0019

[1]To whom correspondence should be addressed at Center of Molecular and Translational Medicine (CMTM) Institution of Biomedical Science (IBMS), Georgia State University (GSU) Petit Research Center, 100 Piedmont Ave, Atlanta, GA 30303. Fax: (404) 413-9566. E-mail: hqiu@gsu.edu.

ABSTRACT

Stress-induced mitochondrial calcium (Ca^{2+}) overload is a key cellular toxic effectors and a trigger of cardiomyocyte death during cardiac ischemic injury through the opening of mitochondrial permeability transition pore (mPTP). We previously found that the valosin-containing protein (VCP), an ATPase-associated protein, protects cardiomyocytes against stress-induced death and also inhibits mPTP opening *in vitro*. However, the underlying molecular mechanisms are not fully understood. Here, we tested our hypothesis that VCP acts as a novel regulator of mitochondrial Ca^{2+} uptake proteins and resists cardiac mitochondrial Ca^{2+} overload by modulating mitochondrial Ca^{2+} homeostasis. By using a cardiac-specific transgenic (TG) mouse model in which VCP is overexpressed by 3.5 folds in the heart compared to the wild type (WT) mouse, we found that, under the pathological extra-mitochondrial Ca^{2+} overload, Ca^{2+} entry into cardiac mitochondria was reduced in VCP TG mice compared to their little-matched WT mice, subsequently preventing mPTP opening and ATP depletion under the Ca^{2+} challenge. Mechanistically, overexpression of VCP in the heart resulted in post-translational protein degradation of the mitochondrial Ca^{2+} uptake protein 1, an activator of the mitochondria Ca^{2+} uniporter that is responsible for mitochondrial calcium uptake. Together, our results reveal a new regulatory role of VCP in cardiac mitochondrial Ca^{2+} homeostasis and unlock the potential mechanism by which VCP confers its cardioprotection.

Key words: VCP; heart; calcium uptake; mPTP; MICU1.

Acute myocardial infarction (AMI) continues to be one of the leading causes of morbidity, disability, and mortality worldwide. While the ischemic episode poses numerous challenges to the heart, recent developments have shown that reperfusion may also lead to cell damage (Hausenloy and Yellon, 2013). Pathological cardiac calcium overload in the mitochondria, which began during ischemia and further exacerbated during reperfusion, is found to be a key cellular toxic effector and a trigger of cardiomyocyte death through the opening of the mitochondrial permeability transition pore (mPTP) (Baines, 2009; Halestrap and Pasdois, 2009; Ong *et al.*, 2015; Perez and Quintanilla, 2017). Thus, preventing excessive Ca^{2+} entering mitochondria serves as a promising target in pursuing protection against cardiomyocyte death caused by ischemia/reperfusion (I/R) damage.

One of the major conduits of Ca^{2+} uptake into the mitochondria is the mitochondria Ca^{2+} uniporter (MCU) (Santo-Domingo

© The Author(s) 2019. Published by Oxford University Press on behalf of the Society of Toxicology.
All rights reserved. For permissions, please e-mail: journals.permissions@oup.com

and Demaurex, 2010). However, the MCU does not function on its own but being controlled by MCU-associated regulators, among which mitochondrial Ca^{2+} uptake proteins (MICUs) have been raised most attentions; for example, increasing evidence indicates that MICU1 activates the MCU at high Ca^{2+} concentrations, while MICU2 acts as an inhibitor of the MCU at lower Ca^{2+} concentrations (Matesanz-Isabel *et al.*, 2016). These findings highlight the possibility of modulating mitochondrial Ca^{2+}-handling proteins to enhance cell resistance against Ca^{2+} overload during stress, and subsequently inhibit mPTP opening and cell death. Although several MCU-associated regulators have recently been identified (De Stefani *et al.*, 2015), the underlying regulatory mechanisms of mitochondrial Ca^{2+} homeostasis in the heart remain largely unknown.

The valosin-containing protein (VCP), also known as Cdc48 in yeast and p97 plants, belongs to the type II AAA (ATPases-Associated with diverse cellular Activities) protein family, known for their involvement in key cellular activities (Asai *et al.*, 2002; Dai *et al.*, 1998; Egerton *et al.*, 1992; Frohlich *et al.*, 1991; Patel and Latterich, 1998; Pleasure *et al.*, 1993; Rabinovich *et al.*, 2002; Schulte *et al.*, 1994). Increased expression of VCP is correlated to growth and viability of cancer cells, highlighting the importance of VCP for cell survival (Tsujimoto *et al.*, 2004; Yamamoto *et al.*, 2003, 2005). We previously demonstrated that overexpressing VCP confers protection on cardiomyocytes against stress-induced apoptosis *in vitro* (Lizano *et al.*, 2013), as well as dramatically reduces infarct size of I/R *in vivo* in cardiac-specific VCP transgenic (TG) mice when compared to wild type (WT) controls (Lizano *et al.*, 2017). We also found that VCP overexpression inhibits mPTP opening both in intact cardiomyocytes and in mitochondria isolated from heart tissues of VCP TG mice (Lizano *et al.*, 2017). However, the underlying mechanisms have not yet been resolved.

Based on our previous studies and other's findings, our present study hypothesized that VCP presents a novel regulator of mitochondrial Ca^{2+} uptake proteins and resists cardiac mitochondrial Ca^{2+} overload by modulating mitochondrial Ca^{2+} homeostasis. By using a cardiac-specific VCP TG mouse model which has shown cardiac protection against I/R injury, we revealed that VCP decreases Ca^{2+} entry cardiac mitochondria under the pathological Ca^{2+} overload, protects against ATP depletion, and modulates the expression of MCU regulators post-translationally.

MATERIALS AND METHODS

Animal model

A TG mouse (FVB) with cardiac-specific overexpression of VCP was generated and characterized as previous described (Zhou *et al.*, 2017). At 2–4 months of age, male and female VCP TG mice were studied alongside litter-matched WT mice as controls. All animal procedures were performed in accordance with the NIH guidance (Guide for the Care and Use of Laboratory Animals, revised 2011) and the protocols were approved by the Institutional Animal Care and Use Committee of Loma Linda University.

Mitochondrial isolation from heart tissues

In order to compare our findings with our previous studies, mitochondria were isolated from mouse left ventricular tissue as previously described (Koentges *et al.*, 2015; Lizano *et al.*, 2017; Qiu *et al.*, 2011). Briefly, left ventricular tissue was homogenized in a buffer (220 nmol/L mannitol 220, 70 nmol/L sucrose, 10 nmol/L 4-(2-hydroxyethyl)-1-piperazineethanesulfonic acid (HEPES), 2 nmol/L ethylene glycol-bis(β-aminoethyl ether)-N,N,N′,N′-tetraacetic acid (EGTA), and pH 7.4 at 4°C) supplemented with 0.25% bovine serum albumin and protease inhibitors (cOmplete™, Roche), using a Potter-Elvehjem glass homogenizer. After an initial spin at 100 × g (5 min) to discard the cellular debris and unbroken cells, the nuclear fraction was pelleted at low-speed centrifugation (1000 × g, 5 min). The supernatant was further centrifuged (10 000 × g, 10 min) to pellet the mitochondrial fraction. The resulting supernatant was ultra-centrifuged (100 000 × g, 90 min) to obtain the cytosolic fraction (supernatant) and a microsomal fraction (pellet). The mitochondrial pellet was resuspended in storage buffer (220 nmol/L mannitol 220, 70 nmol/L sucrose, 10 nmol/L HEPES, pH 7.4 at 4°C). All other pellets were washed 3 times with 1× phosphate-buffered saline and resuspended in radioimmunoprecipitation assay buffer (RIPA buffer) [150 mM NaCl, 1% NP40, 0.5% deoxycholate, 0.1% SDS, 50 mM Tris (pH 8.0)] (Lizano *et al.*, 2017). The purification of the isolated mitochondria from heart tissue was verified by Western blotting, using glyceraldehyde 3-phosphate dehydrogenase (GAPDH, cytosol), Lamin C (nucleus), and voltage-dependent anion channel (VDAC, mitochondria) as loading controls.

Mitochondrial calcium homeostasis assays under Ca^{2+} overloading

Isolated mitochondria (37.5 μg) were resuspended in buffer (120 mM KCl, 10 mM Tris-HCl, 5 mM 3-(N-morpholino)propanesulfonic acid (MOPS), 5 mM Na_2HPO_4, 10 mM glutamate, and 2 mM malate) in a total volume of 150 μl. The isolated mitochondria were then stimulated with higher doses of Ca^{2+} at 50 mM in the buffer in the absence or presence of cyclosporin A (CSA) and the Ca^{2+} retention capacity (CRC) assay was used to measure mPTP opening by using a membrane permeant Ca^{2+} indicator, Rhod-2 AM. Another membrane impermeant Ca^{2+} Green-5N (5 μM; Molecular Probes, Eugene, Oregon) was used to measure extra-mitochondrial Ca^{2+} when the isolated mitochondria were treated with a series of doses of Ca^{2+} pulses (from 2.5 μM to 175 μM) in the absence or presence of CSA (Nguyen *et al.*, 2011). Uptake rates were defined as the change Ca-5N fluorescence in mitochondrial medium compared to the blank buffer which contained no mitochondria ((Fb − F)/Fb), where F refers to fluorescence and b refers to blank control.

ATP production

Mitochondrial ATP production was measured using the Molecular Probes' ATP determination kit (A22066) which uses a convenient bioluminescence assay for quantitative determination of ATP with recombinant firefly luciferase and its substrate D-luciferin. A reaction solution was made according to manufacturer's instructions. Mitochondria were isolated as described previously and energized in the prepared reaction solution with 10 mM glutamate/5 mM malate. A standard curve was established with known concentrations of ATP (0 μM–500 μM), then the reaction was started in the mitochondrial preparations by the addition of adenosine diphosphate (ADP). The fluorescence was measured with a fluorimeter (i3max, Molecular Devices).

RNA *extraction and real-time* PCR

RNA was extracted from isolated left ventricular tissue by using the Quick-RNA MiniPrep kit (Genesee Scientific, San Diego, California) according to the manufacturer's instruction. RNA concentration was determined through photometric measurement on the Nanodrop 2000 (Peqlab, Erlangen, Germany). Quantitative real-time PCR was performed on a CFX96 Touch™ Real-Time PCR Detection System by using iTaq™ Universal

SYBR® Green Supermix (Bio-Rad, Hercules, California) according to the manufacturer's manual. All real-time PCR experiments were performed in triplicate (Zhou et al., 2017).

Protein extraction and subcellular fraction

Following collection and homogenization of left ventricular tissue, total protein was extracted using Tissue Extraction Reagent I (Cat No. FNN0071, Life Technologies Corporation, Grand Island, New York). Subcellular fractionation was achieved by differential centrifugation. After an initial spin at 100 × g (5 min) to discard the cellular debris and unbroken tissue, the nuclear fraction was pelleted at low-speed centrifugation (500 × g, 10 min). The supernatant was further centrifuged (10 000 × g, 10 min) to pellet the mitochondrial fraction. The resulting supernatant was ultra-centrifuged (100 000 × g, 90 min) to obtain the cytosolic fraction (supernatant) and a microsomal fraction (pellet). All pellets were washed 3 times with 1× phosphate-buffered saline and resuspended in RIPA buffer (150 mM NaCl, 1% NP40, 0.5% deoxycholate, 0.1% SDS, and 50 mM Tris (pH 8.0)) (Lizano et al., 2017).

Co-immunoprecipitation (Co-IP) and Western blot

Total protein was extracted then measured by Western blotting and detected using a LI-COR Odyssey® Infrared Imaging System (Lincoln, Nebraska) as previously described (Rashed et al., 2015; Zhou et al., 2017). IP was performed by using the Dynabeads protein G kit (Life Technologies Corporation). Briefly, the primary antibody (Ab) was resuspended with total protein (Ag) and incubated overnight at 4°. The dynabeads were then incubated with the samples overnight to form the Dynabeads-Ab-Ag complex. The tubes were then placed on the magnets and the supernatant was removed. The Dynabeads-Ab-Ag complexes were washed three times using washing buffer (Life Technologies Corporation). Finally, the dynabeads-Ab-Ag complexes were resuspended in elution buffer (Life Technologies Corporation) and 20 μL of eluate was added to the loading dye for Western blot experiments. Western blots were quantitated using the ImageJ software version 1.51, available April, 2018.

Proteasome activity

The chymotrypsin-like activity of the proteasome was measured with the fluorogenic substrate Suc-LLVY-AMC (Boston Biochem, Cambridge, Massachusetts) and fluorescence detected with a Turner TD-700 fluorometer (Turner Designs, Sunnyvale, California).

Cell culture, transfection, and treatments

H9C2 cells were grown in Dulbecco's modified Eagle's medium (DMEM) (Invitrogen), supplemented with 10% fetal bovine serum (FBS) (Invitrogen). We generated an adenovirus harboring a hairpin targeting the VCP sequence for silencing VCP (Si-VCP-Ad). VCP knockdown was performed by transfecting Si-VCP-Ad in H9C2 cell for 48 h with a standard procedure as previously described (Qiu et al., 2011) and a non-relevant short hairpin against luciferase was used for control experiments, as before (Qiu et al., 2011). These cells were further treated with cycloheximide (CHX, 100 μg/ml), which blocks mRNA translation, for different time periods as indicated, with either the absence or the presence of 10 μM MG132 for 2 h before cell lysis. Dimethylsulfoxide (DMSO) was used as a vehicle control for the drug treatment. Cells harvested at the starting point have been considered for the basal level of the protein.

Statistical analysis

Results are presented as the mean ± SEM for the number of samples indicated in the figure legends, where $n = 5$ means that 5 mice were used per group. One-way ANOVA or two-way ANOVA was used to test for significance between groups. Student-Newman-Keuls post hoc correction was applied for multiple pairwise comparisons. A value of $p < .05$ was considered statistically significant.

RESULTS

Overexpression of VCP in the Mouse Heart Prevents Calcium Overload-Induced mPTP Opening

We previously showed that overexpression of VCP in the heart reduced mPTP opening in isolated mitochondria by using an indirect measurement based on the mitochondrial morphological changes under Ca^{2+} stimulation (Lizano et al., 2017). To further reveal the effects of VCP on mitochondrial Ca^{2+} dynamics during Ca^{2+} stress, here we measured the Ca^{2+} levels retained inside the mitochondria upon stimulating mPTP opening using a membrane permeant Ca^{2+} indicator.

To maximally induce mPTP opening, mitochondria isolated from both VCP TG and their litter-matched WT mice were exposed to a high concentration of $CaCl_2$ at 50 mM to exaggerate extramitochondrial Ca^{2+} overload. We then examined the intramitochondrial Ca^{2+} levels by using a known membrane permeant dye, Rhod-2 AM. As shown in Figure 1A, despite adding Ca^{2+}, no Rhod-2 AM fluorescence was detected in our blank control where mitochondria were absent, confirming the specificity of Rhod-2 AM in measuring intramitochondrial Ca^{2+}. We found that, under exposure to 50 mM Ca^{2+}, mitochondria from VCP TG mice exhibited higher Ca^{2+} retention in the mitochondria compared with their litter-matched WTs, reflected by a higher fluorescence of Rhod-2 AM in the mitochondria from VCP TG mice compared with WTs (Figure 1A). We further determined whether the mPTP were fully opened in the mitochondrial of WT mice by repeating the stimulation with two additions of $CaCl_2$ at 50 mM. There were no more changes in Rhod-2 AM fluorescence in WT mice upon the additional Ca^{2+} stimulation, while the Rhod-2 AM fluorescence in VCP TG mice showed a delayed decrease with these additional stimulation, indicating that the mitochondria isolated from VCP TG mice exhibited higher tolerance to high Ca^{2+} challenge.

In addition, pharmacological blockage of mPTP opening using CSA, a known inhibitor of mPTP (Halestrap and Pasdois, 2009; Nguyen et al., 2011), resulted in similar levels of mitochondrial calcium retention between WT and VCP, indicating inhibiting effects of CSA on mPTP opening in both groups (Figure 1A). Importantly, the effect of CSA on WT mitochondria was similar to the results obtained from VCP TG mitochondria without CSA at the first 50 mM Ca^{2+}, highlighting that overexpression of VCP in the heart inhibits Ca^{2+} overloading stimulated by mPTP opening. Furthermore, CSA treatments showed a further inhibition on VCP TG mice at the two additional prolonged stimulations (Figure 1A). These data may also suggest that the mechanism whereby VCP confers its effects was different to those induced by CSA.

We also used Ca^{2+} Green™-5N (Ca-5N), a known membrane-impermeant probe, to detect the change of extra-mitochondrial Ca^{2}. Upon the addition of 50 mM Ca^{2+}, there was a dramatic increase in the Ca-5N fluorescence in the mitochondria from both VCP TG and WT mice compared with the blank buffer control (ie buffer containing no mitochondria), indicating that there was Ca^{2+} efflux from the mitochondria into the buffer upon the high

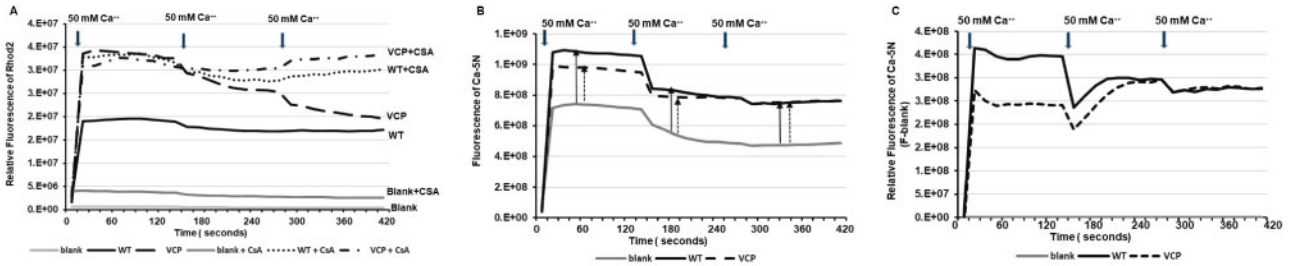

Figure 1. Valosin-containing protein (VCP) inhibits mitochondrial permeability transition pore (mPTP) under extensive calcium-overloading. A, The relative change of the fluorescence level of Rhod2 (indicator of Ca^{2+} inside mitochondria) in samples during the additions of 50 mM Ca^{2+} in the mitochondria isolated from wild type (WT) and VCP transgenic (TG) mice, compared to the blank buffer without mitochondria, upon the absence or presence of mPTP inhibitor [cyclosporin A, (CSA)]. Blank is the control buffer with the same amount of Ca^{2+} loading as the measured samples but without mitochondria. B, The increase of fluorescence of Ca-green-5N (indicator of Ca^{2+} outside mitochondria) in the samples compared to the blank control. C, The relative fluorescence of Ca-green-5N of the mitochondrial samples (F) from the blank buffer (Blank).

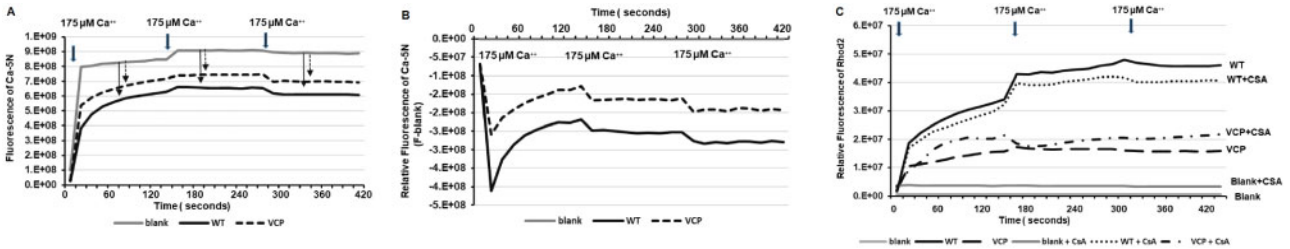

Figure 2. Valosin-containing protein (VCP) resists mitochondrial Ca^{2+} overload via inhibiting Ca^{2+} uptake. The changes of fluorescence of Ca-green-5N (indicator of Ca^{2+} outside mitochondria) in the samples compared to the blank control, during the additions of 175 μM Ca^{2+} in the mitochondria isolated from wild type (WT) and VCP transgenic (TG) mice. B, The decrease of fluorescence of Ca-green-5N of the mitochondrial samples (F) from the blank buffer (Blank). C, The relative change of the fluorescence level of Rhod2 (indicator of Ca^{2+} inside mitochondria) in samples during the additions of 175 μM Ca^{2+} in the mitochondria isolated from wild type (WT) and VCP transgenic (TG) mice, compared to the blank buffer without mitochondria, upon the absence or presence of mPTP inhibitor [cyclosporin A, (CSA)].

Ca^{2+} stimulation (Figs. 1B and 1C). Notably, this increase was greater in WT compared to VCP TG mice during the first Ca^{2+} stimulation (Figs. 1B and 1C). These data are consistent with less Ca^{2+} inside the mitochondria in WT mice and further confirmed the less mPTP opening in VCP TG versus WT mice.

VCP Resists Ca^{2+} Uptake into Mitochondria Under the Ca^{2+} Overloading

Next, we investigated the potential mechanism by which VCP inhibits mPTP opening. Considering that Ca^{2+} overload due to excessive Ca^{2+} entry into mitochondria is a primary factor triggering mPTP opening, we investigated whether there was a difference in Ca^{2+} uptake between the groups before the fully opening of mPTP. We exposed mitochondria isolated from VCP TG and WT mice to a lower concentration of Ca^{2+} challenge and then measured the changes of Ca^{2+} in the buffer inside and outside the mitochondria.

We first investigated the mitochondrial Ca^{2+} uptake with the addition of 175 μM Ca^{2+} boluses. Under the stimulation of this concentration, extra-mitochondrial Ca^{2+} fluorescence (by Ca-5N) at both WT and VCP TG mice were less than blank buffer, indicating no additional Ca^{2+} out from the mitochondria into the buffer upon this Ca^{2+} stimulation (Figure 2A). Mitochondria from VCP TG mouse hearts showed higher extra-mitochondrial Ca^{2+} fluorescence compared with WT (Figure 2A). After the first bolus, there was a dramatic reduction of Ca-5N fluorescence in both groups, indicating an influx of Ca^{2+} into mitochondria. Compared with WT, mitochondria from VCP TG mouse hearts showed less reduction of extra-mitochondrial Ca^{2+} fluorescence (Figure 2B), indicating less mitochondrial Ca^{2+} entry. This difference between the two groups remained similar after two additional 175 μM Ca^{2+} boluses (Figure 2B).

We then used Rhod-2 AM to measure the intramitochondrial Ca^{2+} levels. As showed in Figure 2C, mitochondria from VCP TG mouse hearts showed lower mitochondrial Ca^{2+} fluorescence compared with WT (Figure 2C), indicating less Ca^{2+} uptake in the mitochondria isolated from VCP TG mice compared with WT mice. Different from the observation in the high Ca^{2+} stimulation in which the mPTP was opened, at this concentration, CSA treatment did not change the intramitochondrial Ca^{2+} fluorescence in both groups (Figure 2C), suggesting that lower concentration of Ca^{2+} inside the mitochondria of VCP TG mice was not due to more mPTP opening, but rather due to the less Ca^{2+} moving into mitochondria. These data indicated that VCP TG resisted Ca^{2+} uptake into mitochondria under the Ca^{2+} overload before the mPTP opening. Together, our data showed a dual effect of VCP on mitochondrial calcium homeostasis under the pathological Ca^{2+} stimulation, eg, preventing mitochondrial Ca^{2+} uptake and inhibiting the mPTP opening.

VCP Regulates Mitochondrial Ca^{2+} Uptake Based on a Range of Ca^{2+} Challenge

Considering the different effects of VCP on mitochondrial calcium homeostasis under the different Ca^{2+} concentrations, we then explored the sensitivity and extent of VCP on resistance to Ca^{2+} loading using a series of doses of Ca^{2+} overload in the isolated cardiac mitochondria. As showed in Figure 3A, there was no difference in Ca^{2+} uptake between VCP TG and WT mice at low concentrations of Ca^{2+} (at 2.5 μM, 5 μM, 7.5 μM, and 10 μM). However, significant inhibition of Ca^{2+} uptake rates were found in mitochondria isolated from VCP TG mice

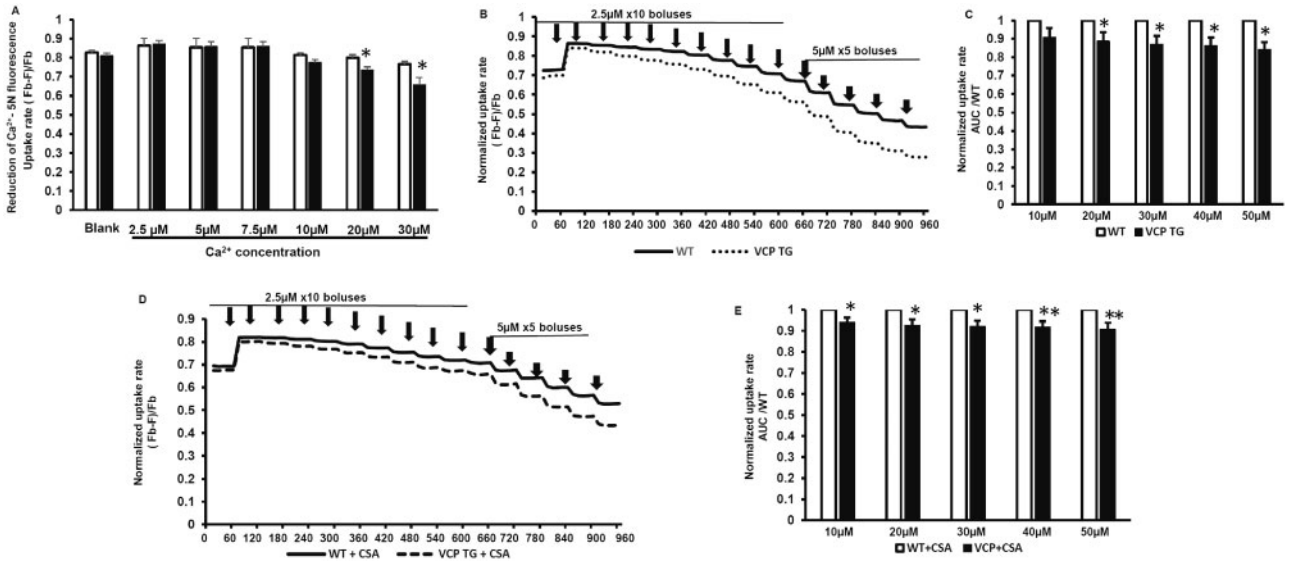

Figure 3. Valosin-containing protein regulates Ca^{2+} uptake into mitochondria varying with a range of Ca^{2+} challenge. A, The relative changes of fluorescence of Ca^{2+}-5N at different doses of Ca^{2+} compared to reading at corresponding blank control. B, The normalized mitochondrial uptake rate, as measured by the relative changes in fluorescence of Ca^{2+}-5N compared to blank control under chronic increase of extra-mitochondrial Ca^{2+}. C, The quantitative average of the area under curves (AUC) of panel B. $n = 5$/group. $^{*}p < .05$, $^{**}p < .01$ versus corresponding wild type (WT). D, The normalized mitochondrial uptake rate in each group under chronic increase of extra-mitochondrial Ca^{2+} in the presence of cyclosporin A (CSA). E, The quantitative average of the AUC of panel D. $n = 4$–5/group. $^{*}p < .05$, $^{**}p < .01$ versus corresponding WT. Abbreviations: F, fluorescence detected in each sample under each bolus of $CaCl_2$; Fb, fluorescence of blank buffer without mitochondria; TG, transgenic, VCP, valosin-containing protein.

compared with WT mice when the concentration of Ca^{2+} was over 20 μM, reflected by decreased reduction in Ca^{2+}-5N fluorescence outside of the mitochondria (Figure 3A).

To further explore the sensitivity of VCP on chronic Ca^{2+} overload, we exposed the isolated mitochondria to Ca^{2+} stimulation using cumulative Ca^{2+} boluses (2.5 μM for 10 times and 5 μM for 5 times (Figure 3B). Mitochondria isolated from VCP TG mouse hearts showed a trend of less mitochondrial uptake than WT mitochondria under this lower Ca^{2+} loading (Figure 3B). Although there is no significant difference in the Ca-5N fluorescence at each bolus of 2.5 μM Ca^{2+} between VCP TG and WT samples, the normalized quantitative Ca^{2+} uptake rate during these repeated additions, as reflected by the area under the curve (AUC), was significantly lower in VCP TG when the cumulative Ca^{2+} was 20 μM or higher (Figure 3D). These data indicate that the mitochondria from VCP TG mice exhibited a progressive resistance to Ca^{2+} overload by reducing the excessive Ca^{2+} entry into mitochondria under Ca^{2+} challenge. In addition, these differences in Ca^{2+} uptake rates between VCP TG and WT mice were not eliminated by the CSA treatment, supporting that the differences in Ca^{2+} fluorescence does not result from changes in mPTP opening, but may be due to the difference of mitochondrial Ca^{2+} uptake between VCP TG versus WT (Figs. 3D and 3E).

VCP Attenuated Ca^{2+} Overload-Induced Mitochondrial Impairment of ATP Production

We next tested whether VCP overexpression altered ATP consumption in isolated mitochondria under Ca^{2+} overload. We used a commercially available luciferase/luciferin kit which utilizes luciferin and ATP produced by the mitochondria to emit light, which can then be read in a luminometer. As shown in Figure 4A, there was no significant difference in ATP levels at baseline with no Ca^{2+} stimulation, suggesting that basal ATP consumption in WT and VCP mitochondria are similar. We then subjected the mitochondria to various concentrations of Ca^{2+} (ranging from 0.05 μM to 100 μM), to determine whether ATP consumption changed during Ca^{2+} uptake. When exposed to Ca^{2+}, ATP levels were significantly decreased in WT cardiac mitochondria. However, this loss of ATP was lower in VCP cardiac mitochondria compared with WT controls (Figure 4B). Significantly less reduction in ATP levels was found in VCP TG samples versus WT samples when mitochondria are placed in 1 μM and 2.5 μM Ca^{2+} (Figure 4C), although there was no difference at the higher concentrations of Ca^{2+}.

We also measured the impairment of ATP production under Ca^{2+} overloading stimulations. When ADP was added to the buffer, mitochondria were pushed towards producing ATP and the resulting luminescence was read. We found that there were no significant differences in the ATP produced by isolated mitochondria from WT and VCP mouse hearts in the absence of Ca^{2+} (Figure 4D). At Ca^{2+} concentrations above 1 μM, ATP production in mitochondria isolated from WT mouse hearts was impaired, compared with baseline. However, this impairment was not observed in VCP TG mitochondria, indicating that the ability to produce ATP was preserved in mitochondria of VCP TG mice under Ca^{2+} overload (Figure 4E).

VCP Regulates Mitochondrial Ca^{2+} Uptake Proteins in the Mouse Hearts

We then determined the molecular mechanisms that were responsible for these alterations of Ca^{2+} handling in the mitochondria in VCP TG mouse hearts. The expression of the mitochondrial Ca^{2+} uniporter (MCU) and its regulators, MICU1 and MICU2, were measured at mRNA levels by qPCR, using freshly extracted heart tissues of both VCP TG and their litter-matched WT mice. As shown in Figure 5A, there were no significant differences in the mRNA levels of MCU, MICU1, and MICU2 between VCP TG and WT mouse hearts, indicating that VCP does not affect the transcription of these genes. We then measured the effect of VCP on these Ca^{2+} handling molecules at the protein level. Mitochondrial fractions of fresh heart tissues were obtained, and as seen in Figures 5B and 5C, overexpression of

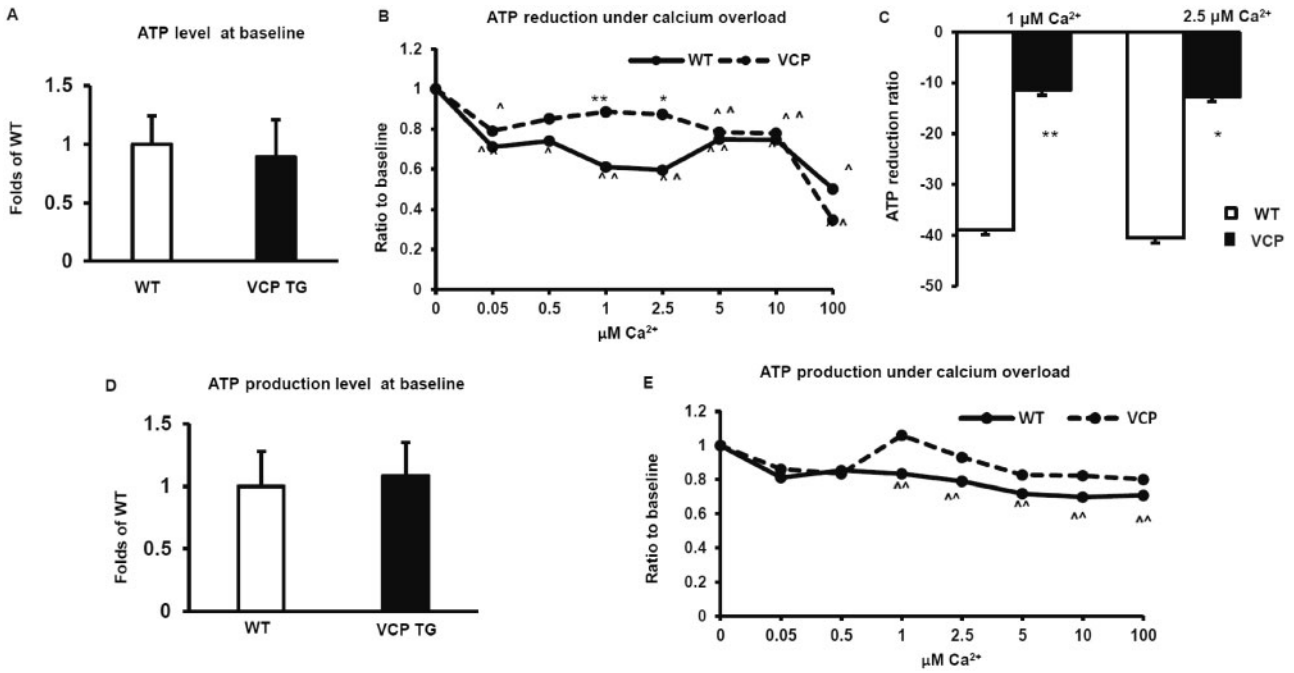

Figure 4. Valosin-containing protein (VCP) attenuates Ca^{2+} overload-induced mitochondrial impairment of ATP production. A, The relative ATP levels at baseline without Ca^{2+} overload in cardiac mitochondria from wild type (WT) and VCP transgenic (TG) mice. $p > .05$ versus WT. $n = 5$–6/group. B, The dose response of ATP levels upon extra-mitochondrial Ca^{2+} stimulation in the absence of ADP. $n = 5$–6/group. $\hat{}p < .05$, $\hat{}\hat{}p < .01$ versus baseline without calcium loading. C, The quantitative average of reduction of ATP levels in mitochondria from VCP TG versus WT under 1 μM and 2.5 μM Ca^{2+} stimulation. $^{*}p < .05$, $^{**}p < .01$ versus WT. D, ATP production upon the addition of ADP with the absence of calcium. E, The dose response of ATP production to extra-mitochondrial calcium overload upon the addition of ADP. $\hat{}\hat{}p < .01$ versus baseline without calcium loading. $N = 6$/group and each sample with triplication.

VCP leads to a ~3.5 fold increase of VCP protein in the mitochondrial fraction from VCP TG mouse hearts versus WT mice. There was no significant difference between VCP TG and WT mice in the protein expression of MCU in the mitochondrial fraction of the hearts (Figs. 5B and 5D). However, we found that the protein level of MICU1, the activator of MCU, was significantly reduced in the mitochondrial fraction of VCP TG mouse heart compared with WT (Figs. 5B and 5E). In addition, we detected two predominant bands of MICU2 in the cardiac mitochondrial fraction, one at about 50 kDa corresponding to the unprocessed precursor (pre-MICU2, upper band), and another faster migrating band at 42 kDa corresponding to the fully processed mature or active form of MICU2 (active MICU2, lower band) (Figure 5B). Compared with WT, VCP TG mice exhibited a significant increase in the mature or active isoform of MICU2 in the mitochondrial fraction while there was no significant difference in the pre-MICU2 expression between the two groups (Figure 5F), resulting in an increase in the ratio of active MICU2/pre-MICU2 (Figure 5F).

VCP Decreases MICU1 by Post-Translational Degradation via Proteasome

Since it has been shown that MICU1 activates the MCU at high Ca^{2+} concentrations while MICU2 inhibits the MCU at lower Ca^{2+} concentrations (Matesanz-Isabel *et al.*, 2016), we focused our attention on investigating the mechanism of the reduction of mitochondrial MICU1 mediated by VCP as most of our data were obtained at concentrations beyond those regulated by MICU2.

Giving the finding that the mRNA of MICU1 are similar between VCP TG and WT mice, we first determined whether the decrease in MICU1 protein in the mitochondria of VCP TG mouse hearts is due to the translocation of MICU1 to other subcellular fractions. Our results showed that, while there was no significant difference in the nuclear fraction between the groups (Figure 6A), MICU1 was also significantly decreased in the cytoplasmic fraction of VCP TG mouse hearts compared with WT (Figure 6B). Together, these data suggest that the decrease in MICU1 expression was not due to the downregulation of synthesis or subcellular translocation but may be due to increased degradation of this protein.

To explore this potential mechanism, we measured the chymotrypsin-like activity of the proteasome, and found proteasome activity was significantly increased in VCP TG samples versus WT mice (Figure 6C). In addition, we measured the abundance of representative components of the proteasome by Western blotting, namely Rpt1 and Rpn2 proteins for the 19S subunit, and α6 proteins for the 20S subunit, and found that these proteasome components were significantly increased in the VCP TG samples compared with WT (Figure 6D).

We further investigated whether VCP was necessary for the degradation of MICU1 by the proteasome by using an alternative cardiomyocyte model. To test this aim, we knocked down VCP in H9C2 cells with a Si-VCP Adenovirus (Si-VCP Ad). As showed in Figure 6E, addition of this adenovirus to H9c2 cells dose-dependently reduced VCP abundance. Since our preliminary results showed that more than 30% decrease of VCP dramatically increased cell death, we used the dose of adenovirus (5MOI) which resulted in 25% decrease of VCP level to treat H9c2 cells and compared it with its control (luciferase) (Figure 6F). A CHX-chase assay was performed in these H9C2 cells to determine the half-life of the MICU1. The Western blotting showed that, while the MCU protein remained unchanged, the treatment of CHX resulted in a rapid degradation of MICU1 through the time course, intracellular levels of MICU1 drastically dropped by more than 50% within 2 h of treatment

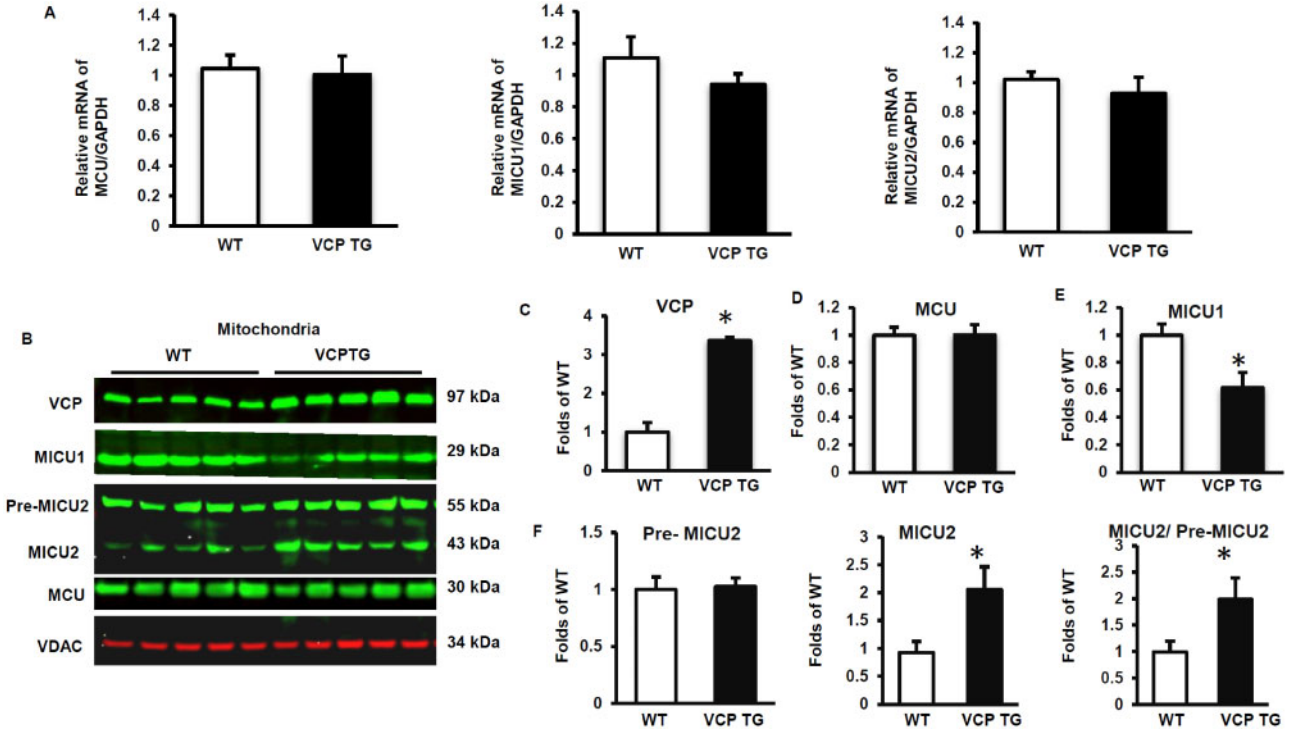

Figure 5. Valosin-containing protein (VCP) regulates mitochondria Ca^{2+} uniporter (MCU) complex in the mouse heart tissue. A, qPCR data show mRNA levels of MCU, MICU1, and MICU2, indicating that overexpression of VCP does not affect transcription of these genes. B–F, Western blot showing protein expression of VCP (C), MCU (D), MICU1 (E), and MICU2 (F) in mitochondrial fractions of heart tissues. $^*p < .05$ versus wild type (WT). $N = 5$/group. Abbreviations: GADPH, glyceraldehyde 3-phosphate dehydrogenase; TG, transgenic; VDAC, voltage-dependent anion channel;

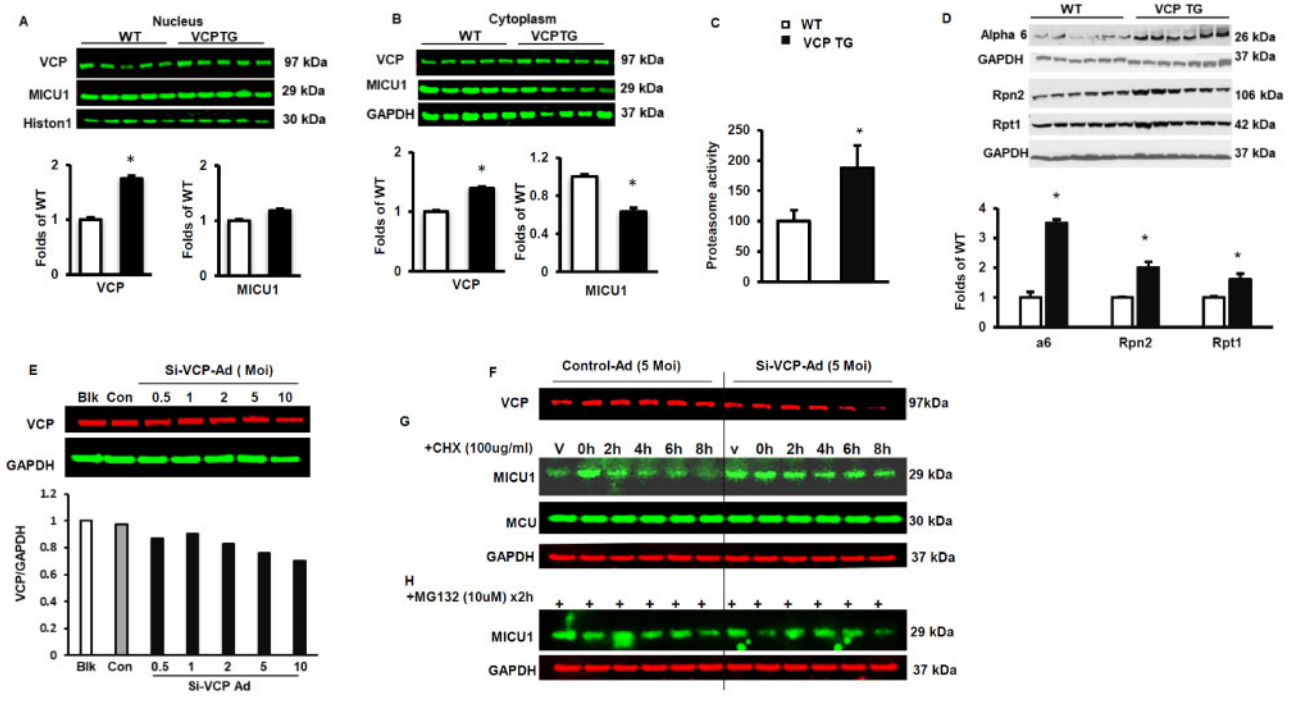

Figure 6. Valosin-containing protein (VCP) increases MICU1 degradation via proteasome. A and B, Subcellular distribution of MICU1 in the mouse heart tissue. Western blot showing protein expression of VCP and MICU1 in nuclear fractions (A) and cytoplasmic fractions (B) $^*p < .05$ versus wild type (WT). $N = 5$/group. C, Overexpression of VCP increases proteasome activity in heart tissues of VCP transgenic (TG) mice versus WT mice. $N = 4$/group with triplication in each samples $^*p < .05$ versus WT. D, Western blot showing protein expression of key components of the Proteasome: a6, Rpn2, and Rpt 1. $N = 6$/group. $^*p < .05$ versus WT. E, Western blotting showing a dose response of the reduction of VCP in H9ce cell upon the knock down of VCP by a Si-VCP adenovirus versus control. F, VCP protein levels in H9C2 cells upon the addition of 5 MOI Si-VCP Ad. G, A cycloheximide (CHX)-chase assay showing half-life of MICU1 and MCU in H9C2 cells upon 5 MOI Si-VCP Ad versus controls. H, Representative Western blots showing MICU1 levels with the treatment of proteasome inhibitor (MG132) in CHX-treated cells for 2 h. Glyceraldehyde 3-phosphate dehydrogenase (GAPDH) was used as loading control of the total proteins from the cells.

(Figure 6G). However, knockdown of VCP dramatically attenuated the degradation of MICU1, which was comparable to the effect of the proteasome inhibitor MG132 in CHX-treated cells (Figure 6H). These results indicate that MICU1 was rapidly and selectively degraded by proteasome in a VCP-dependent manner.

VCP Selectively Facilitates the Degradation of the Ubiquitinated MICU1

Considering the results described above, we further investigated the mechanisms by which VCP specifically modulates MICU1 degradation. Co-IP was performed with the total lysate of heart tissues from both VCP TG and WT mice by using specific anti-MICU1 antibody, and the resulting Western blot was probed with an anti-ubiquitin antibody to detect the ubiquitinated MICU1. The membrane was also probed with an anti-MICU1 antibody as control. As showed in Figure 7A, the ubiquitinated MICU1proteins was remarkably decreased in hearts of VCP TG mice versus WT, which was likely due to the rapid degradation by the increased proteasome activity in VCP TG mouse heart. In another direction, ubiquitin was also immunoprecipitated from whole cell lysate and was probed with an anti-MICU1 antibody to detect the co-immunoprecipitated MICU1. Our results showed a similar reduction in the ubiquinated MICU1 (Figure 7B).

In addition, we measured VCP's effect on Parkin, a known specific regulator of MICU1 degradation (Matteucci *et al.*, 2018). There was no difference in Parkin expression at both mRNA and protein levels between VCP TG and WT mice (Figs. 7C and 7D), indicating that overexpression of VCP does not affect the expression of Parkin. We then tested whether there is any protein-protein interactions among VCP and Parkin. We found that, although there is no direct interaction between VCP and MICU1, Parkin interacted with VCP (Figure 7E). These data together, indicate that VCP may mediate degradation of ubiquitinated MICU1 via interaction with Parkin.

DISCUSSION

Increasing evidence demonstrates that excessive mPTP opening plays a central role in mediating both the necrotic and apoptotic components of I/R injury, particularly at the onset of reperfusion (Garcia-Dorado *et al.*, 2009; Heusch *et al.*, 2010). The present study provides direct evidences highlighting that VCP protects mouse cardiac mitochondria against Ca^{2+} overload-induced mPTP opening by measuring the calcium retained within the mitochondria, which further supported our previous studies *in vitro* in cardiomyocytes and confirmed our previous measurements of the swelling assay, which depends on the morphological change of mitochondria to indirectly reflect mPTP opening. In addition, the results from the present study further revealed a new role of VCP on resisting mitochondrial Ca^{2+} overload through preventing excessive Ca^{2+} entry into mitochondria. Furthermore, our study also established a molecular mechanistic link between the VCP and the regulation of Ca^{2+} uptake proteins. Together, our findings in this study not only revealed a novel regulator of Ca^{2+} homeostasis in the cardiac mitochondria against Ca^{2+} overload but also offered a potential explanation for the mechanism for the VCP-mediated inhibition of mPTP opening and cardiac protection against cell death that we previously observed in isolated cardiomyocytes and in the VCP TG mouse (Lizano *et al.*, 2013, 2017).

Although calcium (Ca^{2+}) is critical to the cardiac mitochondrial function under physiological conditions, excessive mitochondrial Ca^{2+} induced by stress has been founded to be toxic (Konstantinidis *et al.*, 2012; Santulli *et al.*, 2015). It has been shown that excessive mitochondrial Ca^{2+} entry is a primary factor triggering mPTP opening during IR, resulting in the loss of the ability of mitochondria to generate ATP (Wong *et al.*, 2012), eventually leading to I/R-induced cell death (Finkel *et al.*, 2015). Therefore, resisting excessive Ca^{2+} entering mitochondria is essential for cellular adaptation in response to cardiac stress, such as the conditions of AMI or I/R injury. To determine the mechanisms by which VCP inhibits mPTP opening, we then measured Ca^{2+} uptake into isolated mitochondria before the mPTP fully opened. We found that mitochondria from VCP TG mouse hearts exhibited a less mitochondrial Ca^{2+} and a much higher extra-mitochondrial Ca^{2+} levels compared with WT control. Since higher levels of extra-mitochondrial calcium can be due to both decreased mitochondrial Ca^{2+} influx and increased mitochondrial Ca^{2+} efflux, to resolve the potential contribution of mPTP opening to this increase in extra-mitochondrial Ca^{2+} levels, we used CSA to inhibit mPTP opening and found that CSA did not attenuate the difference in Ca^{2+} fluorescence in VCP mitochondria compared with WT under low Ca^{2+} overload (175 μM), suggesting that mPTP opening plays a negligible role in this increase of extra-mitochondrial Ca^{2+} and the change is due to lowered mitochondrial uptake. We also noticed that VCP has little effect on Ca^{2+} uptake at low Ca^{2+} stimulation (below 20 μM), but inhibits Ca^{2+} uptake when Ca^{2+} concentrations are 20 μM or higher. In addition to the mPTP opening, the mitochondrial Na^+/Ca^{2+} exchanger may also play a role in Ca^{2+} efflux from mitochondria. However, this Ca^{2+} release is largely dependent on extra-mitochondrial Na^+ or Li^+ stimulation. Since our experimental buffer did not contain Na^+ or Li^+, it is unlikely that increase of extra-mitochondria Ca^{2+} is due to the additional Ca^{2+} efflux through the activation of mitochondrial Na^+/Ca^{2+} exchanger. Therefore, our data indicate that cardiac-specific VCP overexpression resists Ca^{2+} entry into mitochondria, preventing mitochondrial Ca^{2+} overload under Ca^{2+} stress.

Since mitochondrial Ca^{2+} uptake may also affect ATP production in both physiological and pathological conditions (Tarasov *et al.*, 2012), we further investigated whether VCP altered Ca^{2+}-induced ATP consumption and generation in isolated mitochondria. Our results showed that under pathological Ca^{2+} stimulation, mitochondria from VCP TG hearts were protected against the reduction in ATP levels observed in WT mouse cardiac mitochondria, compared with no Ca^{2+}. In addition, the ATP production was significantly impaired under Ca^{2+} overload in WT compared with mitochondria with no Ca^{2+}, as is characteristic of mitochondria experiencing Ca^{2+} overload (Tarasov *et al.*, 2012). However, this Ca^{2+} overload-induced impairment of ATP production was not observed in VCP TG mouse hearts. Instead, the ability to produce ATP was preserved in VCP TG mitochondria under the calcium challenge. The ability to resist ATP depletion and impaired production is vital to mechanisms that protect cardiomyocytes during I/R stress. It is also notable that despite the protective effects observed under Ca^{2+} overload, overexpression of VCP did not affect ATP production in the absence of Ca^{2+}, indicating that VCP's effect is stress-dependent.

Our previous studies have shown that upon VCP overexpression, there is a subsequent increase of VCP in the nucleus of cardiac cells where VCP plays important roles in regulating other gene expressions via signaling pathway involving AKT/NF-κβ/Stat3/iNOS (Lizano *et al.*, 2013). We believed that the increased nuclear expression of VCP was also linked to the translocation of VCP to the mitochondria where it conferred its

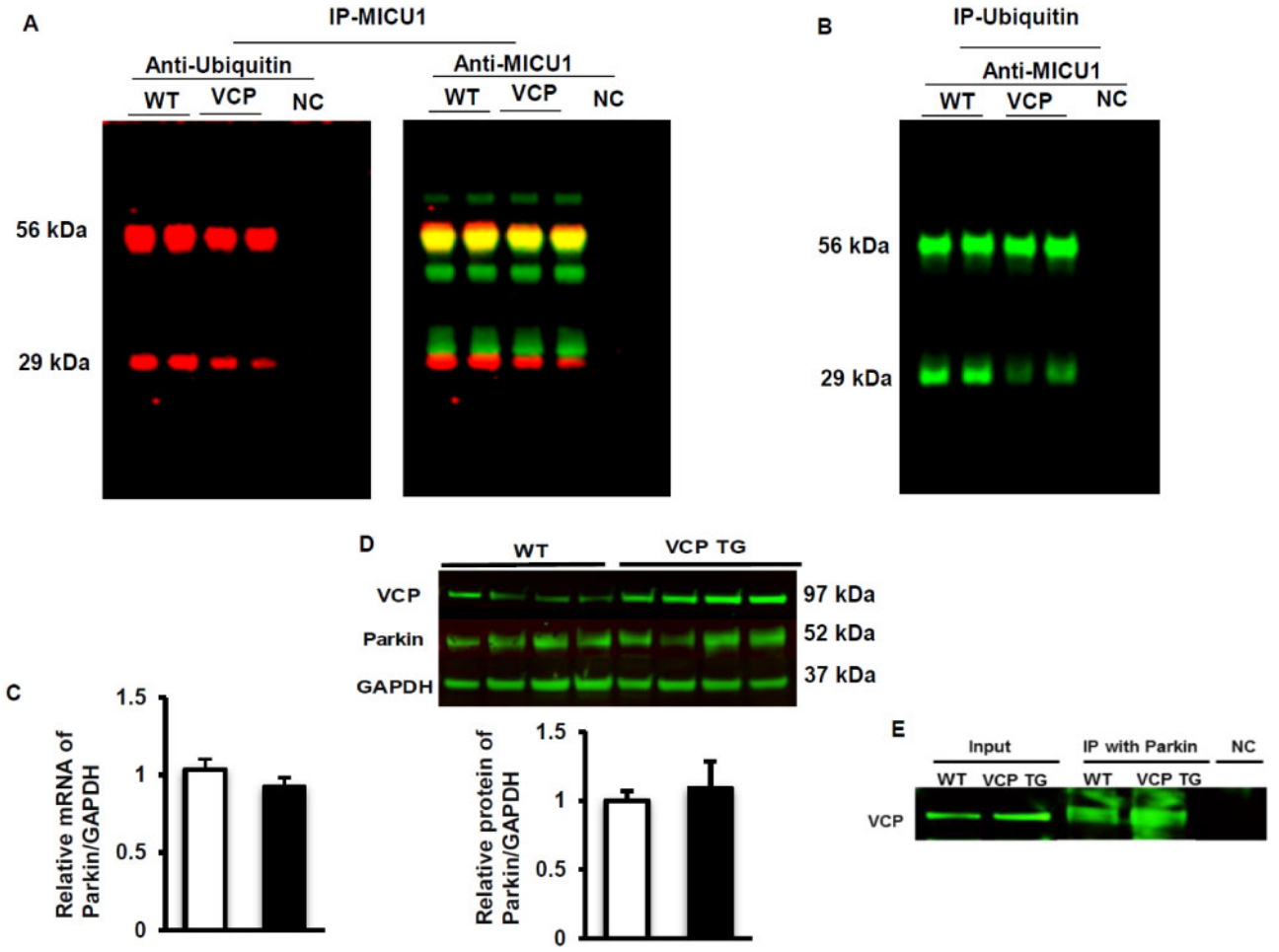

Figure 7. Valosin-containing protein (VCP) selectively mediates ubiquitinated MICU1 degradation. A, Co-immunoprecipitation (co-IP) of the total lysate of heart tissues from both VCP transgenic (TG) and wild type (WT) mice by using specific anti-MICU1 antibody, and probed with an anti-ubiquitin antibody and anti-MICU1 antibody. B, Co-immunoprecipitation (co-IP) of the total lysate of heart tissues from both VCP TG and WT mice using specific anti-ubiquitin antibody, and probed with an anti-MICU1 antibody. C, mRNA of Parkin in mouse heart tissue measured by qPCR. D, Protein expression of Parkin measured by Western blotting. E, Western blotting showing the protein interaction between VCP and Parkin after IP with Parkin antibody. Abbreviations: GADPH, glyceraldehyde 3-phosphate dehydrogenase; NC, negative control.

effects on mitochondrial function as we observed in our previous studies (Lizano *et al.*, 2017) and in this study. There is a general consensus that mitochondrial Ca^{2+} uptake is mediated by the MCU complex (Santo-Domingo and Demaurex, 2010), a multi-subunit Ca^{2+} channel complex whose expression may vary depending on the cell type, subtype, and even Ca^{2+} stimulation (Markus *et al.*, 2016). Although the precise molecular composition of the cardiac MCU complex is still being studied, a few proteins have been identified, particularly: the pore-forming protein MCU, its regulatory heterodimer composed by the stimulatory component MICU1, the inhibitory component, MICU2 (Matesanz-Isabel *et al.*, 2016), and essential MCU regulator (EMRE), a single-pass membrane protein that links MCU and MICU1 together (Nemani *et al.*, 2018). Since the MCU complex is a major mode of mitochondrial Ca^{2+} influx, inhibiting its activity poses as an attractive means to prevent Ca^{2+} overload, mPTP opening, and subsequent cardiomyocyte death (Kwong, 2017). Our results from this study demonstrated that VCP participates in the regulation of the MCU complex via a comprehensive mechanism. First, we noticed that there is no significant difference of MCU level at both mRNA and protein levels between the VCP TG and WT mice, indicating that the effect of VCP on the mitochondrial Ca^{2+} uptake was not due to the reduction of mitochondria number or the formation of MCU pores. Second, overexpression of VCP in the heart significantly decreases the protein expression of MICU1 in mitochondrial fraction compared with WT. Third, VCP TG mice exhibited a significant increase in the active MICU2 (42 kDa) with no difference at pre-MICU2 levels when compared with WT, and no difference at mRNA levels of MICU2 between the two groups. These data indicate that VCP may modify the MICU2 at the post-translational level in the heart without altering the transcription level.

Considering that MICU1 plays a major role on the regulation of MCU at high Ca^{2+} levels while MICU2 regulates MCU at the lower Ca^{2+} level (<7 μm) (Matesanz-Isabel *et al.*, 2016), it is reasonable to assume that the VCP-mediated modulation of mitochondrial Ca^{2+} homeostasis observed in our experiments were more likely due to the changes in MICU1 since the Ca^{2+} levels was out of the range for triggering MICU2 function. As such, we further investigated the potential mechanisms by which VCP decreased MICU1 in the mitochondria. There are some possibilities that VCP may reduce MICU1 in the mitochondrial fraction, including the decrease of MICU1 synthase, intracellular redistribution and degradation of the proteins. Our data

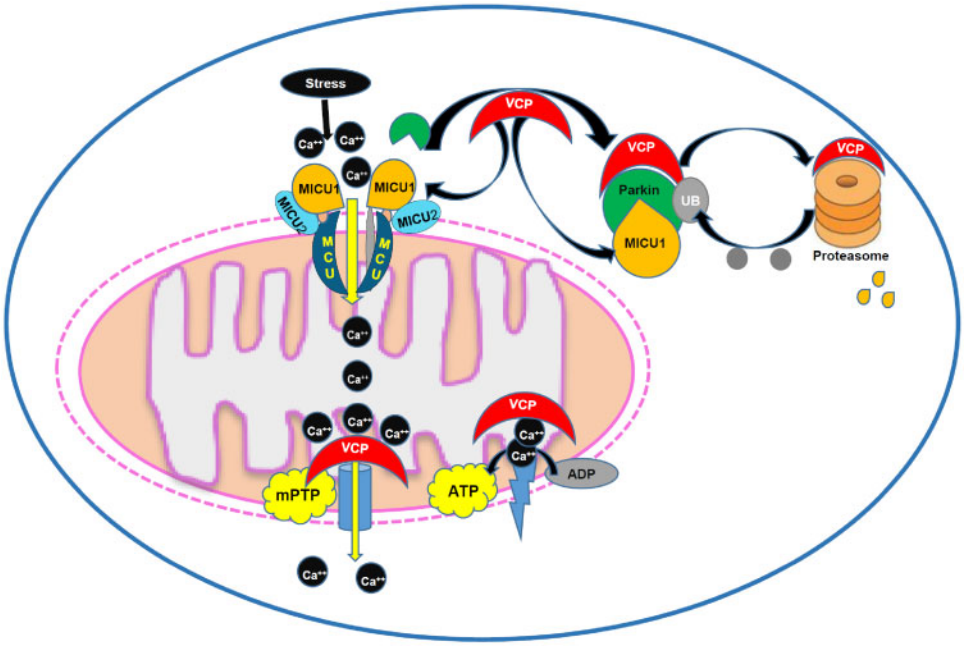

Figure 8. Summary of the findings. The results from this study indicate a new role of valosin-containing protein (VCP) on mitochondrial Ca^{2+} homeostasis through inhibiting Ca^{2+} uptake, preventing mitochondrial permeability transition pore (mPTP), and subsequently resisting Ca^{2+} challenge. Mechanistically, VCP regulates mitochondrial Ca^{2+}-handling by decreasing the MCU activator, MICU1, through the increase of degradation of this protein.

showed that there is no difference of MICU1 mRNA level between the two groups, no increase of MICU1 in other cellular fractions. Instead, MICU1 was significantly decreased in the cytoplasm while no significant difference was seen in the nuclear fraction. These data together suggested that the decrease of MICU1 in the mitochondrial fraction in VCP TG mouse hearts is not the result from the decrease of protein synthesis or from intracellular redistribution of the protein, but rather may result from increased degradation of MICU1. Our data further confirmed that overexpression of VCP dramatically increased both proteasome abundance and activity compared with WT. Although a universal mechanism underlying the regulation of proteasome expression remains elusive, recent studies have identified a transcription factor nuclear factor erythroid-derived 2-related factor 1 (NFE2L1, also known as Nrf1) was identified to be a pivotal regulator promoting the expression of all proteasome subunits in mammals. Interestingly, studies in other cells demonstrated that the activation of Nrf1 depends on VCP, by which VCP not only helps Nrf1 extracted from the endoplasmic reticulum (ER), but also contributes to Nrf1 proteolytic processing to release Nrf1's active region and allow it to be translocated to the nucleus, where it becomes transcriptionally active (Motosugi and Murata, 2019; Radhakrishnan *et al.*, 2010, 2014; Sha and Goldberg, 2014). In addition, our data showed that MICU1 is short-lived protein and is degraded in a VCP-dependent manner since impaired VCP remarkably delayed the degradation of MICU1. Since the ubiquitin-proteasome system (UPS) is the most important mechanism of proteolysis in the heart (Lilienbaum, 2013; Zheng and Wang, 2010), these data support that VCP acts as an integral component of the ubiquitin/proteasome pathway and play a role in the regulation of MCU complex function through the protein degradation via promoting UPS activity.

Our results indicate a selective degradation of MICU1 in VCP TG mice. While the underlying mechanisms need to be further explored, there are several possibilities for this effect of VCP: first, in addition to the increase of proteomic activity, VCP also facilitates the extraction of ubiquitinated proteins in various subcellular location and chaperons them to the proteasome, which is necessary for these proteins' degradation (Xu *et al.*, 2011). For example, it has been shown that Parkin, a 465-residue E3 ubiquitin ligase, was recruited to mitochondria and ubiquitinated proteins at the OMM. A recent study has demonstrated that Parkin directly participates in the selective regulation of MICU1 by acting as a scaffold for the proteasome-mediated degradation of MICU1 (Matteucci *et al.*, 2018). Interestingly, VCP was also found to be recruited at mitochondria by parkin (Narendra *et al.*, 2008; Pickrell and Youle, 2015). Our data in the VCP TG mouse model further showed that parkin interacted with both MICU1 and VCP, an interaction may result in the selective degradation of ubiquitinated MICU1 in mitochondria. Secondly, VCP can also remodel proteins in OMM which may contribute to its selective regulatory effect in protein quality control (Heidelberger *et al.*, 2018). Thirdly, it was also shown that VCP can act as an alternate subunit of proteasomes by interacting with the 20S Peptidase to form an ATP-powered proteasome (Meyer and Weihl, 2014; Tran and Brodsky, 2014), which may provide an additional explanation to the increased proteasome activity in TG mice and may also result in a selective effect on the degradation on the proteins that were bound to it.

It has been known that the majority mitochondrial proteins imported from the nuclei and cytosol undergo a proteolytic cleavage by the mitochondrial processing peptidase (MPP), which is necessary for the maturation of the pre-proteins to their functional forms in mitochondria. Although MICU2 maturation in mitochondria was observed in a recent report (Matteucci *et al.*, 2018) and in our present study, the mechanism underlying the processing is yet unclear. We noticed that there was no physical direct interaction between VCP and MICU2 proteins (data not shown), we speculate that VCP likely functions

through binding other proteins (its cofactors) that can specifically bind and recognize the targeting signal of MICU2, resulting in a proteolytic cleavage on MICU2 by MPP, thus lead to its maturation in cardiac mitochondria. It might be also hypothetical that VCP-mediated decrease of MICU1 interrupts the formation of the MICU1/MICU2 heterodimers, which may stimulate the adaptive recruitment of MICU2 to mitochondria and lead to a secondary MICU2 maturation.

In summary, as also illustrated in the Figure 8, our results from this study revealed a new role of VCP on mitochondrial Ca^{2+} homeostasis through inhibiting Ca^{2+} uptake, preventing mitochondrial Ca^{2+} overload, and subsequently resisting Ca^{2+} challenge. Mechanistically, VCP regulates mitochondrial Ca^{2+}-handling by decreasing the MCU activator, MICU1, through the increase of degradation of this protein. These results, together with our previous studies, indicate that VCP presents a novel regulator of Ca^{2+} homeostasis in mitochondria that leads to the prevention of mPTP opening and cardiac protection against I/R injury.

DECLARATION OF CONFLICTING INTERESTS

The authors declared no potential conflicts of interest with respect to the research, authorship, and/or publication of this article.

Funding

The National Institutes of Health (NIH) (HL115195-01 to H.Q., HL137962 to H.Q., and HL142291 H.Q. and G.Q.).

Author Contributions

H.Q., S.S., and G.Q. made substantial contributions to conceptual design, acquisition of data, analysis, and interpretation of data, and have been involved in drafting and revising the manuscript critically for important intellectual content. S.S. performed all the measurement of mitochondrial Ca^{2+} regulation and Western blotting and qPCR. J.X. performed IP and Western blotting as well as data analysis. B.M. performed *in vitro* experiments on cells and Co-IP on heart tissues. C.L. contributed to animal and experimental support, data analysis, and interpretation. E.J.B. contributed to Ca^{2+} uptake experiments, data analysis, and interpretation.

References

Asai, T., Tomita, Y., Nakatsuka, S., Hoshida, Y., Myoui, A., Yoshikawa, H., and Aozasa, K. (2002). VCP (p97) regulates NFkappaB signaling pathway, which is important for metastasis of osteosarcoma cell line. *Jpn. J. Cancer Res.* **93**, 296–304.

Baines, C. P. (2009). The mitochondrial permeability transition pore and ischemia-reperfusion injury. *Basic Res. Cardiol.* **104**, 181–188.

Dai, R. M., Chen, E., Longo, D. L., Gorbea, C. M., and Li, C. C. (1998). Involvement of valosin-containing protein, an ATPase Co-purified with IkappaBalpha and 26 S proteasome, in ubiquitin-proteasome-mediated degradation of IkappaBalpha. *J. Biol. Chem.* **273**, 3562–3573.

De Stefani, D., Patron, M., and Rizzuto, R. (2015). Structure and function of the mitochondrial calcium uniporter complex. *Biochim. Biophys. Acta* **1853**, 2006–2011.

Egerton, M., Ashe, O. R., Chen, D., Druker, B. J., Burgess, W. H., and Samelson, L. E. (1992). VCP, the mammalian homolog of cdc48, is tyrosine phosphorylated in response to T cell antigen receptor activation. *EMBO J.* **11**, 3533–3540.

Finkel, T., Menazza, S., Holmström, K. M., Parks, R. J., Liu, J., Sun, J., Liu, J., Pan, X., and Murphy, E. (2015). The ins and outs of mitochondrial calcium. *Circ. Res.* **116**, 1810–1819.

Frohlich, K. U., Fries, H. W., Rudiger, M., Erdmann, R., Botstein, D., and Mecke, D. (1991). Yeast cell cycle protein CDC48p shows full-length homology to the mammalian protein VCP and is a member of a protein family involved in secretion, peroxisome formation, and gene expression. *J. Cell Biol.* **114**, 443–453.

Garcia-Dorado, D., Ruiz-Meana, M., and Piper, H. M. (2009). Lethal reperfusion injury in acute myocardial infarction: facts and unresolved issues. *Cardiovasc. Res.* **83**, 165–168.

Halestrap, A. P., and Pasdois, P. (2009). The role of the mitochondrial permeability transition pore in heart disease. *Biochim. Biophys. Acta* **1787**, 1402–1415.

Hausenloy, D. J., and Yellon, D. M. (2013). Myocardial ischemia-reperfusion injury: a neglected therapeutic target. *J. Clin. Invest.* **123**, 92–100.

Heidelberger, J. B., Voigt, A., Borisova, M. E., Petrosino, G., Ruf, S., Wagner, S. A., and Beli, P. (2018). Proteomic profiling of VCP substrates links VCP to K6-linked ubiquitylation and c-Myc function. *EMBO Rep.* **19**, e44754.

Heusch, G., Boengler, K., and Schulz, R. (2010). Inhibition of mitochondrial permeability transition pore opening: the holy grail of cardioprotection. *Basic Res. Cardiol.* **105**, 151–154.

Koentges, C., Konig, A., Pfeil, K., Holscher, M. E., Schnick, T., Wende, A. R., Schrepper, A., Cimolai, M. C., Kersting, S., Hoffmann, M. M., *et al.* (2015). Myocardial mitochondrial dysfunction in mice lacking adiponectin receptor 1. *Basic Res. Cardiol.* **110**, 495.

Konstantinidis, K., Whelan, R. S., and Kitsis, R. N. (2012). Mechanisms of cell death in heart disease. *Arterioscler. Thromb. Vasc. Biol.* **32**, 1552–1562.

Kwong, J. Q. (2017). The mitochondrial calcium uniporter in the heart: energetics and beyond. *J. Physiol.* **595**, 3743–3751.

Lilienbaum, A. (2013). Relationship between the proteasomal system and autophagy. *Int. J. Biochem. Mol. Biol.* **4**, 1–26.

Lizano, P., Rashed, E., Kang, H., Dai, H., Sui, X., Yan, L., Qiu, H., and Depre, C. (2013). The valosin-containing protein promotes cardiac survival through the inducible isoform of nitric oxide synthase. *Cardiovasc. Res.* **99**, 685–693.

Lizano, P., Rashed, E., Stoll, S., Zhou, N., Wen, H., Hays, T. T., Qin, G., Xie, L. H., Depre, C., and Qiu, H. (2017). The valosin-containing protein is a novel mediator of mitochondrial respiration and cell survival in the heart in vivo. *Sci. Rep.* **7**, 46324.

Markus, N. M., Hasel, P., Qiu, J., Bell, K. F., Heron, S., Kind, P. C., Dando, O., Simpson, T. I., and Hardingham, G. E. (2016). Expression of mRNA encoding MCU and other mitochondrial calcium regulatory genes depends on cell type, neuronal subtype, and Ca^{2+} signaling. *PLoS One* **11**, e0148164.

Matesanz-Isabel, J., Arias-del-Val, J., Alvarez-Illera, P., Fonteriz, R. I., Montero, M., and Alvarez, J. (2016). Functional roles of MICU1 and MICU2 in mitochondrial Ca(2+) uptake. *Biochim. Biophys. Acta* **1858**, 1110–1117.

Matteucci, A., Patron, M., Reane, D. V., Gastaldello, S., Amoroso, S., Rizzuto, R., Brini, M., Raffaello, A., and Cali, T. (2018). Parkin-dependent regulation of the MCU complex component MICU1. *Sci. Rep.* **8**, 14199.

Meyer, H., and Weihl, C. C. (2014). The VCP/p97 system at a glance: connecting cellular function to disease pathogenesis. *J. Cell Sci.* **127**, 3877–3883.

Motosugi, R., and Murata, S. (2019). Dynamic regulation of proteasome expression. *Front. Mol. Biosci.* **6**, 30.

Narendra, D., Tanaka, A., Suen, D. F., and Youle, R. J. (2008). Parkin is recruited selectively to impaired mitochondria and promotes their autophagy. *J. Cell Biol.* **183**, 795–803.

Nemani, N., Shanmughapriya, S., and Madesh, M. (2018). Molecular regulation of MCU: implications in physiology and disease. *Cell Calcium* **74**, 86–93.

Nguyen, T. T., Stevens, M. V., Kohr, M., Steenbergen, C., Sack, M. N., and Murphy, E. (2011). Cysteine 203 of cyclophilin D is critical for cyclophilin D activation of the mitochondrial permeability transition pore. *J. Biol. Chem.* **286**, 40184–40192.

Ong, S. B., Samangouei, P., Kalkhoran, S. B., and Hausenloy, D. J. (2015). The mitochondrial permeability transition pore and its role in myocardial ischemia reperfusion injury. *J. Mol. Cell Cardiol.* **78**, 23–34.

Patel, S., and Latterich, M. (1998). The AAA team: related ATPases with diverse functions. *Trends Cell Biol.* **8**, 65–71.

Perez, M. J., and Quintanilla, R. A. (2017). Development or disease: duality of the mitochondrial permeability transition pore. *Dev. Biol.* **426**, 1–7.

Pickrell, A. M., and Youle, R. J. (2015). The roles of PINK1, parkin, and mitochondrial fidelity in Parkinson's disease. *Neuron* **85**, 257–273.

Pleasure, I. T., Black, M. M., and Keen, J. H. (1993). Valosin-containing protein, VCP, is a ubiquitous clathrin-binding protein. *Nature* **365**, 459–462.

Qiu, H., Lizano, P., Laure, L., Sui, X., Rashed, E., Park, J. Y., Hong, C., Gao, S., Holle, E., Morin, D., *et al.* (2011). H11 kinase/heat shock protein 22 deletion impairs both nuclear and mitochondrial functions of STAT3 and accelerates the transition into heart failure on cardiac overload. *Circulation* **124**, 406–415.

Rabinovich, E., Kerem, A., Frohlich, K. U., Diamant, N., and Bar-Nun, S. (2002). AAA-ATPase p97/Cdc48p, a cytosolic chaperone required for endoplasmic reticulum-associated protein degradation. *Mol. Cell Biol.* **22**, 626–634.

Radhakrishnan, S. K., den Besten, W., and Deshaies, R. J. (2014). p97-dependent retrotranslocation and proteolytic processing govern formation of active Nrf1 upon proteasome inhibition. *eLife* **3**, e01856.

Radhakrishnan, S. K., Lee, C. S., Young, P., Beskow, A., Chan, J. Y., and Deshaies, R. J. (2010). Transcription factor Nrf1 mediates the proteasome recovery pathway after proteasome inhibition in mammalian cells. *Mol. Cell* **38**, 17–28.

Rashed, E., Lizano, P., Dai, H., Thomas, A., Suzuki, C. K., Depre, C., and Qiu, H. (2015). Heat shock protein 22 (Hsp22) regulates oxidative phosphorylation upon its mitochondrial translocation with the inducible nitric oxide synthase in mammalian heart. *PLoS One* **10**, e0119537.

Santo-Domingo, J., and Demaurex, N. (2010). Calcium uptake mechanisms of mitochondria. *Biochim. Biophys. Acta* **1797**, 907–912.

Santulli, G., Xie, W., Reiken, S. R., and Marks, A. R. (2015). Mitochondrial calcium overload is a key determinant in heart failure. *Proc. Natl. Acad. Sci. USA* **112**, 11389–11394.

Schulte, R. J., Campbell, M. A., Fischer, W. H., and Sefton, B. M. (1994). Tyrosine phosphorylation of VCP, the mammalian homologue of the Saccharomyces cerevisiae CDC48 protein, is unusually sensitive to stimulation by sodium vanadate and hydrogen peroxide. *J. Immunol.* **153**, 5465–5472.

Sha, Z., and Goldberg, A. L. (2014). Proteasome-mediated processing of Nrf1 is essential for coordinate induction of all proteasome subunits and p97. *Curr. Biol.* **24**, 1573–1583.

Tarasov, A. I., Griffiths, E. J., and Rutter, G. A. (2012). Regulation of ATP production by mitochondrial Ca(2+). *Cell Calcium* **52**, 28–35.

Tran, J. R., and Brodsky, J. L. (2014). The Cdc48-Vms1 complex maintains 26S proteasome architecture. *Biochem. J.* **458**, 459–467.

Tsujimoto, Y., Tomita, Y., Hoshida, Y., Kono, T., Oka, T., Yamamoto, S., Nonomura, N., Okuyama, A., and Aozasa, K. (2004). Elevated expression of valosin-containing protein (p97) is associated with poor prognosis of prostate cancer. *Clin. Cancer Res.* **10**, 3007–3012.

Wong, R., Steenbergen, C., and Murphy, E. (2012). Mitochondrial permeability transition pore and calcium handling. *Methods Mol. Biol.* **810**, 235–242.

Xu, S., Peng, G., Wang, Y., Fang, S., and Karbowski, M. (2011). The AAA-ATPase p97 is essential for outer mitochondrial membrane protein turnover. *Mol. Biol. Cell* **22**, 291–300.

Yamamoto, S., Tomita, Y., Nakamori, S., Hoshida, Y., Nagano, H., Dono, K., Umeshita, K., Sakon, M., Monden, M., and Aozasa, K. (2003). Elevated expression of valosin-containing protein (p97) in hepatocellular carcinoma is correlated with increased incidence of tumor recurrence. *J. Clin. Oncol.* **21**, 447–452.

Yamamoto, S., Tomita, Y., Uruno, T., Hoshida, Y., Qiu, Y., Iizuka, N., Nakamichi, I., Miyauchi, A., and Aozasa, K. (2005). Increased expression of valosin-containing protein (p97) is correlated with disease recurrence in follicular thyroid cancer. *Ann. Surg. Oncol.* **12**, 925–934.

Zheng, Q., and Wang, X. (2010). Autophagy and the ubiquitin-proteasome system in cardiac dysfunction. *Panminerva Med.* **52**, 9–25.

Zhou, N., Lee, J. J., Stoll, S., Ma, B., Costa, K. D., and Qiu, H. (2017). Rho kinase regulates aortic vascular smooth muscle cell stiffness via actin/SRF/myocardin in hypertension. *Cell Physiol. Biochem.* **44**, 701–715.

Zhou, N., Lee, J. J., Stoll, S., Ma, B., Wiener, R., Wang, C., Costa, K. D., and Qiu, H. (2017). Inhibition of SRF/myocardin reduces aortic stiffness by targeting vascular smooth muscle cell stiffening in hypertension. *Cardiovasc. Res.* **113**, 171–182.

Zhou, N., Ma, B., Stoll, S., Hays, T. T., and Qiu, H. (2017). The valosin-containing protein is a novel repressor of cardiomyocyte hypertrophy induced by pressure overload. *Aging Cell* **16**, 1168–1179.